INSTITUTE OF PLASMA PHYSICS

NAGOYA UNIVERSITY

Particle Loss from Magnetic Cusp Field

C. Namba, T. Kawamura and H. Obayashi

IPPJ-209 December 1974

RESEARCH REPORT

NAGOYA, JAPAN

Particle Loss from Magnetic Cusp Field

C. Namba, T. Kawamura and H. Obayashi

IPPJ-209 December 1974

Further communication about this report is to be sent to the Research Information Center, Institute of Plasma Physics, Nagoya University, Nagoya, Japan.

Abstract

The motion of charged particles in an axially symmetric magnetic field of cusp configuration is studied by means of numerical calculations. A particular attention is paid to a non-adiabatic zone. The computer results are compared with a simplified loss cone model and it is shown that there is a critical value of non-adiabaticity parameter which defines an effective size of the non-adiabatic zone.

§1. Introduction

A plasma in a magnetic cusp configuration is known stable in the M.H.D. sense, though its loss is rather fast through the magnetic open ends, i.e., the line and point cusps. Recently it is suggested and demonstrated by Sato et al[1] that these end losses are well suppressed by an additional rf fields applied at the cusp ends. This is referred to as the rf plugging effect and is also investigated theoretically by Watanabe and Hatori.[2]

In order to understand and estimate the plugging effect in a quantitative way, it is first necessary to study the behaviour of the plasma in a static magnetic cusp without applying any rf field. This is, in itself, quite interesting and important a problem of plasma physics[3-4] and particle dynamics[5-9], because of its particular geometry and the essential non-adiabaticity associated with B=0.

From this point of view, we have made a computational analysis of the motion of charged particles in an axially symmetric cusp field, and investigated the nature and extent of a non-adiabatic zone in the phase space. A particular attention is paid to the final state of particles, i.e., to how the initial velocity distribution defines the final particle-escape patterns through the cusp necks.

§2. Simple Cusp Field

Let us consider an axially symmetric magnetic field of cusp configuration which is described by the stream function

$$\psi = -r^2 z, \qquad (1)$$

in a cylindrical coordinate system (r, θ, z). Here the units of length, L_0, and magnetic field strength, B_0, are understood. The components and total strength of the field are given by

$$B_r = r \ ,$$

$$B_z = -2z \ , \qquad (2)$$

and $$B = (r^2 + 4z^2)^{1/2} \ .$$

The motion of a single charged particle with mass m and charge e is investigated. Taking the unit of time $\tau_0 \equiv mc/eB_0$, we have a simple equation of motion

$$\frac{d\vec{v}}{dt} = \vec{v} \times \vec{B} \ . \qquad (3)$$

Since the magnetic field is static and axially symmetric, we have two constants of motion, the total velocity v and the total angular momentum P_θ. For the particle coming close to the origin (r=0,z=0), where the magnetic field vanishes, the magnetic moment is no a conserved quantity, and it behaves non-adiabatically. This effect can be represented by a parameter:

$$\kappa \equiv \rho \frac{|\nabla B|}{B} = v\sqrt{\frac{r^2 + 16z^2}{(r^2 + 4z^2)^3}} \ , \qquad (4)$$

which implies the relative change of the magnetic field over a gyroradius $\rho = v/B$. In the region where κ is small enough the motion is considered adiabatic. Apart from the vicinity of r- or z-axis, κ is of the same order as $\lambda = \rho/R$, where R is the magnetic radius of curvature. In Fig.1 some characteristic contours of the field are given.

Along a fixed line of force $|\psi| = \psi_c$, the field strength takes its minimum value $B_c = \sqrt{3}\ \psi_c^{1/3}$ at $|z| = (1/2)\psi_c^{1/3}$, $r^2 = 2\ \psi_c^{2/3}$, so that there we have

$$\kappa = \sqrt{2}\ v/B_c^2 = \frac{\sqrt{2}\ v}{3\ \psi_c^{2/3}} \qquad (5)$$

§3. Particle Injection from Null Field

As we are interested in the non-adiabatic effect on the particle motion, a special consideration is done for the particle injection from the null field point. Now the total angular momentum around the z-axis vanishes and the magnetic moment cannot be defined.

In order to see he particle escape through the cusp necks, i.e., two point cusps along the z-axis and a line cusp around the z-axis, the equation of motion (1) is integrated numerically with varying initial velocity vectors and fixed initial position. The computation program was developed according to the Runge-Kutta-Gill method. The initial velocity space (v_r, v_z)

is quantized to make square meshes with the step of $\Delta v_r = \Delta v_z = 0.01$. Setting the confinement region (the size of device) to be $|x|, |y|, |z| \leq 5$, the integration has been carried out up to $t = 60$.

The result of calculation is mapped in Fig.2-a, where the particle in each cell of initial velocity space is categorized in accordance with the final conditions:

(A) Escaping out through the left point cusp ($z < -5$) before $t = 60$.

(B) Escaping out through the right point cusp ($z > +5$) before $t = 60$.

(C) Escaping out through the line cusp ($|x|, |y| > 5$) before $t = 60$.

(D) Remaining in the confinement region up to $t = 60$.

In Fig.2 (showing only $v_z > 0$ half plane) we can see the bulk structure of loss cones, i.e., type (B) along positive v_z and type (C) along v_r directions, as well as scattered distributions between these loss cones.

The bulk structures are interpreted as the direct loss from the cusp region. If the parameter κ is meaningful, we can introduce a critical magnetic field intensity by (5)

$$B_c = 2^{1/4} \sqrt{v/\kappa} \ , \qquad (6)$$

and we may define a "non-adiabatic (NA) zone" inside the contour

$$B = B_c \ , \qquad (7)$$

which is an ellipsoide. To reproduce the bulk pattern in Fig.2-a, we make a simple picture of NA zone by assuming the negligible magnetic field. When a particle is injected from $r_0 = z_0 = 0$, with a velocity v at an angle ϕ from z-axis, it will run straightly until it intersects the critical surface with a pitch angle α given by

$$\cos \alpha = \frac{3 \cos^2\phi - 1}{\sqrt{3 \cos^2\phi + 1}} \quad . \tag{8}$$

Since the particle behaves adiabatically outside the NA zone, the condition for escaping through the cusp necks are given as follows:

(A) Loss from the left point cusp:

$$\sqrt{1 - (B_c/B_p)} \leq \cos \alpha \leq 1 , \qquad \cos \phi < 0 .$$

(B) Loss from the right point cusp

$$\sqrt{1 - (B_c/B_p)} \leq \cos \alpha \leq 1 , \qquad \cos \phi > 0 .$$

(C) Loss from the line cusp

$$-1 < \cos \alpha < -\sqrt{1 - (B_c/B_\ell)} \quad .$$

Here, $B_p = 5$, and $B_\ell = 10$ are the field intensities at the corresponding cusp necks. We thus obtain the widths ϕ_p and ϕ_ℓ of the loss cones for the injection:

$$\cos \phi_p = \sqrt{\frac{1}{6}} \{3 - \frac{B_c}{B_p} + \sqrt{(1 - \frac{B_c}{B_p})(9 - \frac{B_c}{B_p})}\}^{1/2}$$
$$\cos \phi_\ell = \sqrt{\frac{1}{6}} \{3 - \frac{B_c}{B_\ell} - \sqrt{(1 - \frac{B_c}{B_\ell})(9 - \frac{B_c}{B_\ell})}\}^{1/2} \tag{9}$$

This simplified loss cone model is compared with the computational results, and we can find in Fig.2-b that the

pattern is well reproduced by the critical value of $\kappa = 1/3 \sim 1/6$. This is very consistent with the estimate of non-adiabaticity by Grad and van Norton, who investigated slightly non-adiabatic cases and estimated the non-adiabaticity parameter of ~ 30 %. It should, however, be remarked that the present treatment is rather confined to the particle behavior deep inside the NA zone, in contrast to Grad and van Norton's case.

For the scattered distribution in Fig.2-a, we can only guess that they are lost after several mirror reflections.

§4. Particle Injection on the Axsis

The same kind of computer calculations as §3 has been carried out for several injection points shifted axially ($r_0 = 0$, $z_0 \neq 0$). Here we have vanishing angular momentum again. The results shown in Fig.3 - 5 are composed of three parts, the bulk loss cones similar to Fig.2 with some distortion, the very remarkable branch patterns, and the scattered or thin structures between them.

For the bulk losses a similar analysis can be applied and understood as well. It is, on the contrary, very difficult to explain the branch patterns and the scattered structure.

The value of κ, however, seems independent of the velocity v. This implies that the critical magnetic field B_c given by (6), and therefore the scale length of any non-adiabatic effect may be proportional to $\sqrt{v}$.

In other words, as far as κ is independent of v, we have a

scaling law

$$L \propto \sqrt{v} \quad . \tag{10}$$

This relation is directly verified by the inspection of Fig.3 - 5, i.e., if we take the velocity scale in these figures to be proportional to z_0^2, the patterns, including the branch structures, are quite similar to one another.

For the branch structures it is very interesting to see that the lifetimes of the particles belonging to the same branch are quite similar. Moreover, if we make orbit trajectories in the coordinate space, the branch particles seem to arrive at the NA zone with nearly the same values of gyration phase angle. We, therefore, may say that these branches are in some sense the diffraciton patterns shown in passing through the NA zone.

§5. *Discussions and Remarks*

The comparison of the semi-quantitative analysis with the computer calculation shows us

(i) that there is an effective boundary of NA zone in the cusped field, approximately defined by $\kappa = 1/3 \sim 1/6$,

(ii) that there is a remarkable scale law given by (10).

(iii) that the branch patterns shown in the cases $z_0 \neq 0$ seem due to the diffraction caused by NA zone..

Here we must add some other remarks:

a) For considering particle confinement in the cusp device it

should be necessary to take the distribution function into account. If, for example, we choose an isotropic Maxwellian distribution with the thermal velocity $v_T = 0.2$ in the case of central injection ($r_0 = z_0 = 0$), the computer result gives the final distribution for $v_r^2 + v_z^2 \leq 1$, $v_z \geq 0$:

(A) 3.7 %

(B) 6.0 %

(C) 30.3 %

(D) 58.5 %

This means that about 60 % of particles remains after t = 60.

b) If we give the factor of normalization, say,

$L_0 = 10$ cm,

and $B_0 = 10$ KG,

then the cusp strengths are

$B_p = 50$ KG at $z = \pm 50$ cm,

$B_p = 100$ KG at $r = 50$ cm,

and the time interval t = 60 corresponds to 0.624 μsec for protons. The velocity scale v = 1 implies about 500 KeV proton kinetic energy.

c) When the initial injection point is not on the z-axis, the total angular momentum P_θ will not in general vanish. In this case we can have the Störmer zone for particle motion. This is also reflected in the patterns in the initial velocity space, but is open for further investigation.

References

1. Sato T. et al., Proceeding of Symposium on Feedback and Dynamic Control of Plasmas,New York (1970) 310.
   Miyake S. et al., J. Phys. Soc. Japan 31 (1971) 265.

2. Watanabe T., and Hatori R., Research Report of Institute of Plasma Phys. Nagoya Univ. Japan IPPJ-132.
   Hatori R. and Watanabe T. Research Report of Institute of Plasma Phys., Nagoya Univ., IPPJ-133.

3. Berkowitz J. et al., Proceeding of the Second International Conf. on the Peaceful Uses of Atomic Energy, Geneva, 31 (1958) 171.

4. Grad H., Phys. Rev. Letters 4 (1960) 222.

5. van Norton R., NYO Report 9495 (1961).
   Grad H. and van Norton R., Nuclear Fusion Suppl. part 1 (1962) 61.

6. Schmidt G., Phys. Fluids 5 (1962) 994.

7. Schuurman W. and de Kluiver H., J. Nucl. Energy Part C (1965) 154.

8. Ito H., Kakuyugo-Kenkyu, Circular in Japanese, 14 (1965) 364.

9. Taylor J.B., CLM Report R58 (1966).

Figure Captions

Fig.1. Characteristic contours of the magnetic field given by $\psi = -r^2 z$.

Fig.2-a. Computed distribution map in initial velocity space for starting point $r_0 = 0$ and $z_0 = 0$. The particle in each cell is categorized in accordance with the final conditions:

(A) Escaping out through the left point cusp ($z < -5$) before $t = 60$.

(B) Escaping out through the right point cusp ($z > 5$) before $t = 60$.

(C) Escaping out through the line cusp ($|x|, |y| > 5$) before $t = 60$.

(D) Remaining in the containment region up to $t = 60$.

⊠ denotes the particle of type (A),

■ —— type (B), ■ —— type (C), and

□ —— type (D).

Fig.2-b. Comparison of the semi-quantitative analysis with the computer calculation shown in Fig.2-a. for several values of κ.

Fig.3. Computed distribution map in initial velocity space for starting point $r_0 = 0$, $z_0 = -1.0$.

Fig.4. Computed distribution map in initial velocity space for starting point $r_0 = 0$, $z_0 = -2.0$.

Fig.5. Computed distribution map in initial velocity space for starting point $r_0 = 0$, $z_0 = -5.0$.

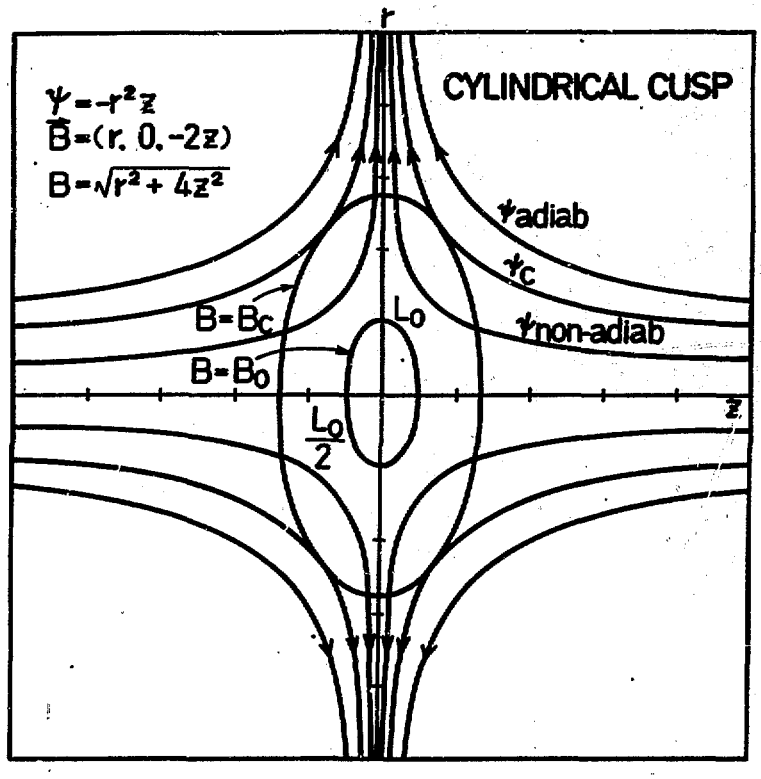
r
CYLINDRICAL CUSP
$\psi = -r^2 z$
$\vec{B} = (r, 0, -2z)$
$B = \sqrt{r^2 + 4z^2}$
ψ_{adiab}
ψ_c
$\psi_{non\text{-}adiab}$
$B = B_c$
$B = B_0$
L_0
$\frac{L_0}{2}$
z

Fig. 1

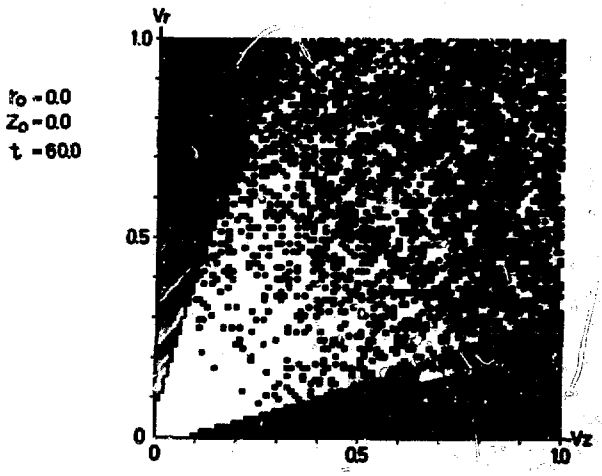
Vr
1.0
0.5
0
0
0.5
1.0
Vz
r_o = 0.0
Z_o = 0.0
t = 60.0

Fig. 2-a

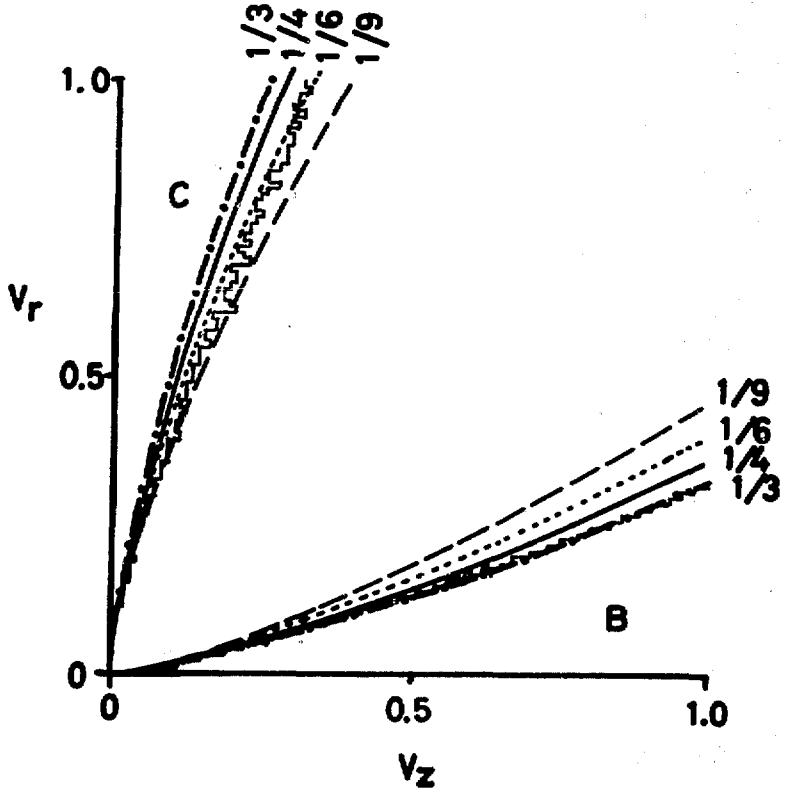
1/3
1/4
1/6
1/9
1.0
C
V_r
0.5
0
0
0.5
1.0
V_z
1/9
1/6
1/4
1/3
B

Fig. 2-b

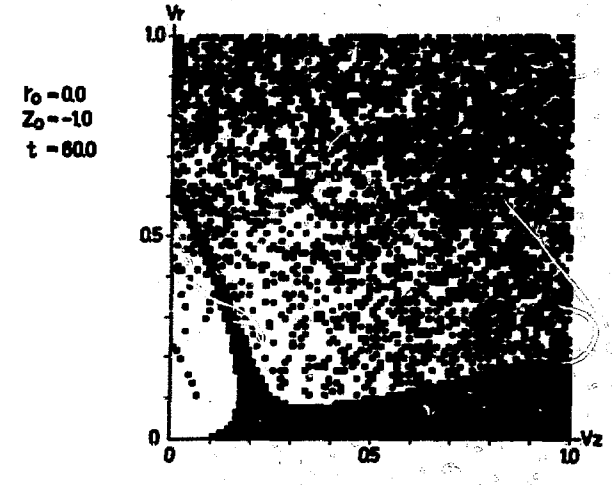

Fig. 3

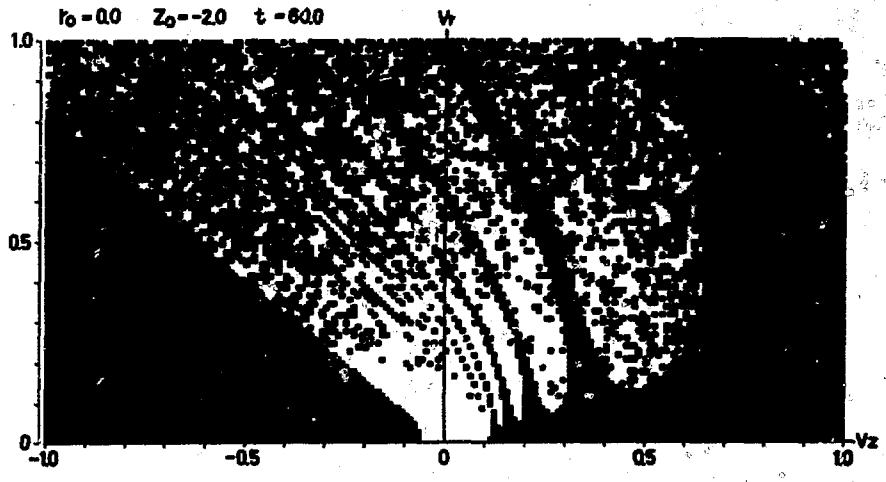

Fig. 4

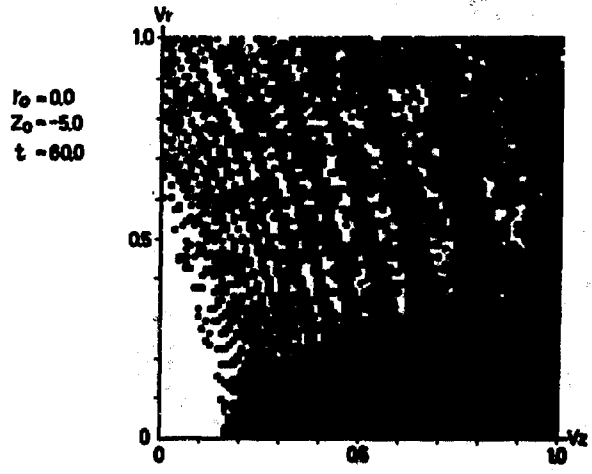

Fig. 5